ACS Medicinal Chemistry Letters

Letter

Spiro-oxindole piperidines and 3-(azetidin-3-yl)-1H-benzimidazol-2-ones as mGlu2 receptor PAMs

Ana Isabel de Lucas, Juan Antonio Vega, Encarnación Matesanz, María Lourdes Linares, Aránzazu García Molina, Gary Tresadern, Hilde Lavreysen, Andrés A. Trabanco, and José María Cid

ACS Med. Chem. Lett., **Just Accepted Manuscript** • DOI: 10.1021/acsmedchemlett.9b00350 • Publication Date (Web): 10 Oct 2019

is published by the American Chemical Society. 1155 Sixteenth Street N.W., Washington, DC 20036

Spiro-oxindole piperidines and 3-(azetidin-3-yl)-1H-benzimidazol-2-ones as $mGlu_2$ receptor PAMs

Ana Isabel de Lucas,[‡,*] Juan Antonio Vega,[‡] Encarnación Matesanz,[‡] María Lourdes Linares,[‡] Aránzazu García Molina, [‡] Gary Tresadern, [§] Hilde Lavreysen, [ǀ] Andrés A. Trabanco, [‡] and José María Cid[‡,*]

[‡] Discovery Chemistry, Janssen Research & Development, Division of Janssen-Cilag S.A., Jarama 75A, Toledo 45007, Spain

[§]Computational Chemistry, Discovery Neuroscience, Janssen Research & Development, Division of Janssen Pharmaceutica NV, Turnhoutseweg 30, B-2340 Beerse, Belgium.

[ǀ]Discovery Neuroscience, Janssen Research & Development, Division of Janssen Pharmaceutica NV, Turnhoutseweg 30, B-2340 Beerse, Belgium

KEYWORDS. Metabotropic glutamate receptor 2, $mGlu_2$, $mGluR_2$, GRM2, positive allosteric modulators, PAMs, scaffold hopping

ABSTRACT: Starting from two weak $mGlu_2$ receptor positive allosteric modulator (PAM) HTS hits (**4** and **5**) a molecular hybridization strategy resulted in the identification of a novel spiro-oxindole piperidine series with improved activity and metabolic stability. Scaffold hopping around the spiro-oxindole core identified the 3-(azetidin-3-yl)-1*H*-benzimidazol-2-one as bioisoster. Medicinal chemistry optimization of these two novel chemotypes resulted in the identification of potent, selective, orally bioavailable and brain penetrant $mGluR_2$ PAMs.

INTRODUCTION

Metabotropic glutamate (mGlu) receptors represent a family of G protein-coupled receptors (GPCRs) that are activated by the excitatory neurotransmitter glutamate.[1,2] To date, eight mGlu receptor subtypes have been identified and classified into 3 groups based on sequence homology, pharmacologic profile and preferential signal transduction pathway.[3] The $mGlu_2$ and $mGlu_3$ receptors are the members of group II that couple negatively to adenylyl cyclase through Gi/Go proteins. Activation of the $mGluR_2$ results in reduced glutamate release and decreases excitability. $mGluR_2$ activation can be achieved with orthosteric agonists or can be modulated by positive allosteric modulation of the receptor. A positive allosteric modulator (PAM) can increase the affinity and/or efficacy of the endogenous neurotransmitter glutamate binding to a site topologically distinct from the orthosteric (glutamate) ligand binding sites. PAMs of $mGluR_2$ have emerged as promising novel therapeutic agents for the treatment of several central nervous system (CNS) disorders.[4-6] The $mGluR_2$ is expressed on presynaptic glutamatergic nerve terminals where it functions as an autoreceptor for glutamate. Thus, a $mGlu_2$ PAM can normalize excessive glutamatergic neurotransmission, which may be of benefit in disorders such as epilepsy[7,8] and schizophrenia.[9,10]

We have previously reported on a series of pyridones originated from a high throughput screening (HTS) campaign of the Addex Pharmaceuticals compound collection.[11]

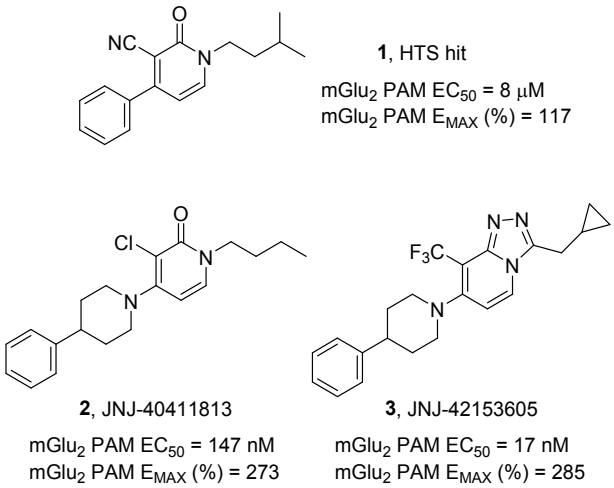

Figure 1. Previously reported $mGlu_2$ PAM hit 1 and subsequent lead molecules 2 and 3.

As previously described, starting from the HTS hit **1** (Figure 1), potency and druglike properties were significantly improved to deliver the clinical lead JNJ-40411813 (**2**).[12] Subsequent back up programs focused on novel chemical series identified by pharmacophore overlays and scaffold hopping using the pyridone core as template.[13-14] Additional leads, such as JNJ-42153605 (**3**),[15,16] with improved potencies and druglike related attributes were found. Later, we confirmed these series bind in the 7-transmembrane domain of the receptor[17] and the discovery of the first covalent PAM, an analogue of **3**, helped confirm our overlay and binding mode hypotheses.[18] Using modeling and mutagenesis a mechanism was proposed for how PAMs initiate their functional effect.[19]

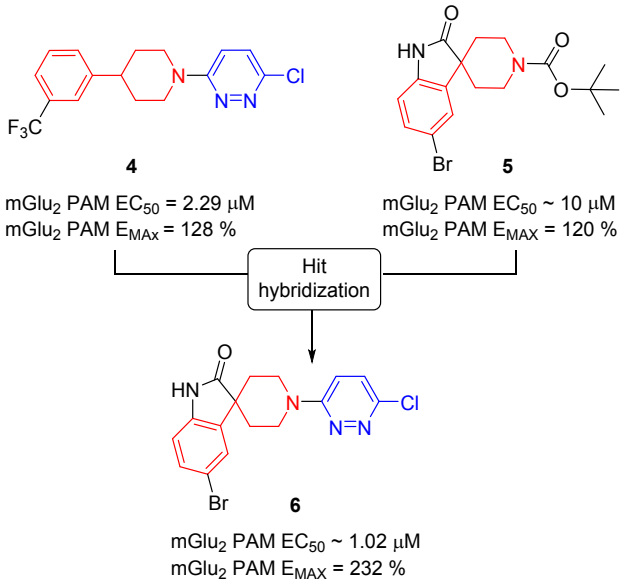

Figure 2. Structure and primary activity of hits 4 and 5 and hybrid molecule 6.

As part of a continuing effort to identify and develop novel $mGluR_2$ PAMs from structurally different scaffolds a second HTS campaign, now using the Janssen compound library, was conducted. Nine hit series with structurally distinct chemotypes were found. Hit triaging using $mGlu_2$ receptor PAM potency and in vitro ADME profiling prioritized two novel series, exemplified by hits **4** and **5** (Figure 2) as the most promising. We hypothesized that the phenylpiperidine motif of hit **4** was embedded into the structure of the spiro-oxindole piperidine hit **5**, suggesting that hybrid analogues could be worth exploring. To validate the hypothesis the hybrid compound **6** was synthesized. Pleasingly, compound **6** showed a two-fold increase in potency with respect to hit **4** (**6**: EC_{50} = 1.02 μM vs **4**: EC_{50} = 2.29 μM) and a significant increase in the E_{MAX} of 232% indicating a substantial increase in the glutamate response. Herein, we report on the synthesis, SAR exploration and medicinal chemistry optimization of this novel series as well as on the initial pharmacokinetic evaluation of selected early leads.

RESULTS AND DISCUSSION The initial exploration of compound **6** focused on two main aspects: study the effect of substituents on the indolone core ring and piridazinyl ring. Functional activity and microsomal stability data for spiro-oxindole piperidine **6** along with new derivatives **7-26** are summarized in Table 1 and 2.

Table 1. Functional activity and metabolic stability data for representative spiro-oxindole piperidine $mGluR_2$ PAMs 6-20

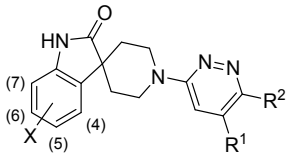

compd	X	R^1	R^2	$mGlu_2$ EC_{50} (nM)[a] (95% CI)	$mGlu_2$ E_{MAX} (%)[b] ± SD	$mGlu_2$ % effect @ 1 μM[b] ± SD	HLM (%)[c]	RLM (%)[c]
6	5-Br	H	Cl	1,020 (822-1257)	232 ± 64	100 ± 17	8	25
7	H	H	Cl	n.d.[d]	217 ± 6	24 ± 13	45	95
8	7-Br	H	Cl	3,090[e]	65 ± 4	9 ± 2	n.t.[e]	n.t.
9	6-Br	H	Cl	n.d.	183 ± 2	76 ± 7	n.t.	n.t.
10	4-Br	H	Cl	n.d.	108[d]	31 ± 5	n.t.	n.t.
11	5-Cl	H	Cl	1,000 (904-1132)	187 ± 14	80 ± 8	8	76
12	5-F	H	Cl	n.d.	184 ± 17	31 ± 4	11	57
13	5-Cy	H	Cl	630 (317-1285)	169 ± 5	105 ± 22	45	100
14	5-Br	H	H	n.d.	141[d]	7 ± 3	n.t.	n.t.
15	5-Br	H	Me	n.d.	228[d]	36 ± 18	17	69
16	5-Br	H	CF_3	400 (242-654)	53 ± 2	46 ± 6	4	20
17	5-Br	H	OEt	>10,000	52 ± 11	5 ± 0	7	31

18	5-Br	NHEt	Cl	240 (110-535)	394[d]	263 ± 18	8	65
19	5-Br	OEt	Cl	210 (150-309)	380[d]	203 ± 42	11	58
20	5-Br	OEt	CF_3	130 (96-164)	216 ± 35	160 ± 23	9	43

[a] Values are the mean of at least two experiments and within confidence interval of >95%. [b] Values are the median of at least two experiments with standard deviation. [c] HLM and RLM data refer to % of compound metabolized after incubation with microsomes for 15 min at a 5 uM concentration. [d] n.d.: absolute EC_{50} could not be calculated since no obvious upper plateau of the concentration-response curve was reached. [e] no tested.

Removing the bromine atom (**7**) from the indolone core led to decrease in potency and worsened metabolism. Moving the bromine atom from C-5 to other positions of the aromatic ring was also detrimental for activity. Thus compound **8** (7-Br) was 3-fold less potent showing a low E_{MAX} and isomers **9** (6-Br) and **10** (4-Br) weakly active. The role of the bromine atom at C-5 was assessed by exploring alternative substituents. For instance, a chlorine substituent was equipotent (**11,** EC_{50} = 1,000 nM), however it displayed higher metabolism in rat liver microsomes (**11**, RLM 76% vs **6**. RLM 25%). The smaller and less lipophilic fluorine (**12**) was not tolerated leading to an inactive molecule. Nevertheless, the $mGluR_2$ PAM activity was recovered with the introduction of the more lipophilic cyclopropyl substituent (**13**) having comparable potency but lacking good stability in both HLM and RLM. Moreover, SAR on the pyridazine ring showed that removing the chlorine atom (**14**) resulted also in a decrease in activity. Next, several replacements for the chlorine group of the pyridazine such as methyl (**15**), trifluoromethyl (**16**), and ethoxy (**17**) were explored. These modifications turned out to be unfavorable leading to either low E_{MAX} (**16**, 53%) or loss of activity (**15** and **17**, %effect at 1 μM 36% for **15** and 5% for **17**, EC_{50} > 10 μM for **17**). Introduction of a second substitution on the pyridazine ring was explored with compounds **18-19**. Incorporation of an ethylamino (**18**) or ethoxy (**19**) adjacent to the chlorine atom led to a ~4 and 5-fold increase in potency respectively compared to **6** but also with some decrease of the metabolic stability in RLM. In the continued effort to find alternatives for the chlorine group of the pyridazine, we went back to the CF_3 group, which resulted in compound **20** having an additional improvement in potency (EC_{50} = 130 nM; E_{MAX} = 216%). Thus compound **20** is ~2-fold more potent than **19** and ~7.5-fold more potent than the initial hit **6**, keeping the in vitro metabolic profile in an acceptable range.

We next focused on finding replacements of the central spiro-oxindole core. To that end, a scaffold hopping exercise looking for non-spirocyclic bicyclic cores was conducted. We applied computational techniques based on 3D shape and electrostatic similarity. Such approaches are well suited to scaffold hopping as similarity is assessed using properties important for biological recognition and not the underlying atom connectivity. We have previously assessed these techniques in detail[20] and applied them to identify $mGlu_2$ PAM scaffolds.[13] Here we performed a similar approach aimed at replacing the central piperidine with alternative secondary amines and we also searched databases of pre-fragmented compounds. The ROCS[21] and EON software from Openeye Scientific[22] were used which assess shape and electrostatic similarity respectively. Amongst the best computational hits was the benzimidazolone core (**21**) with an azetidine substituent, Figure 3. The shape and electrostatic similarity between the two were high suggesting this as a strong candidate for follow-up chemistry.

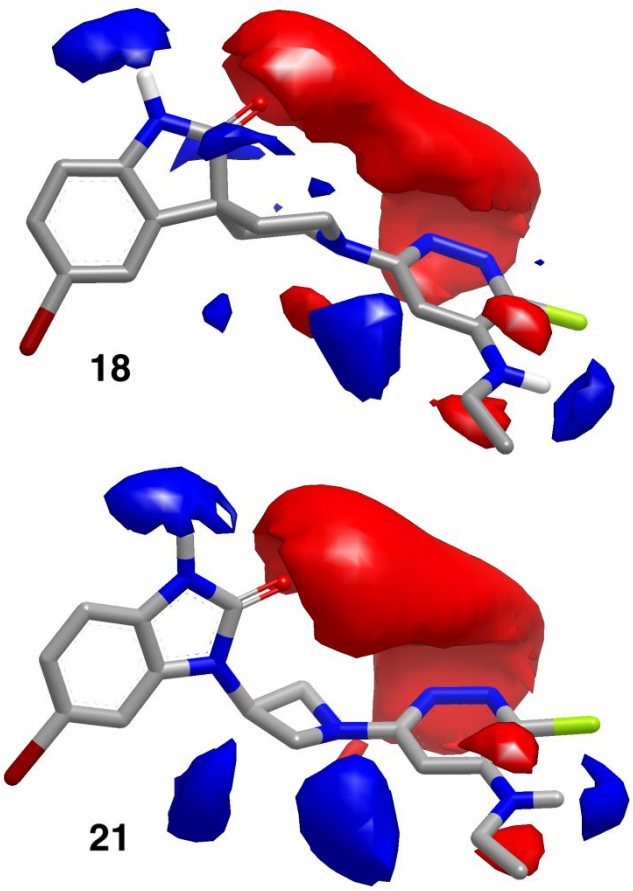

Figure 3. Comparison of the 3D conformation and electrostatic surfaces for spiro-oxindole piperidine (**18**) and a new hit containing a 1H-benzimidazol-2-one core (**21**) with azetidine substitution. The red surface represents region of negative electrostatic charge and the blue surface is positive charge.

The 3-(azetidin-3-yl)-1H-benzimidazol-2-one core exemplified with compound **21**, stood out as an optimal bioisosteric replacement of the spiro-oxindole piperidine. Pleasingly, the new subclass represented by **21** showed comparable $mGlu_2$ PAM activity and interestingly better metabolic stability when compared to its corresponding match pair **18**. This encouraging result triggered a focused exploration in which the 3-(azetidin-3-yl)-1*H*-benzimidazol-2-one core was kept as template to explore SAR on both left- and right-hand side. The most relevant examples prepared along with their primary activity and metabolic stability data are summarized in Table 2. In contrast to the previous subclass, removal of the 6-bromine atom on the benzimidazolone scaffold (**22**) did not have any effect on the potency or the metabolic stability. Replacement of

the pyridazine for pyridine (**23**) resulted in a ~2.3-fold potency increase compared to **22** although the compound was found to be metabolically less stable in both HLM and RLM. Substitution of the aminoethyl group on **23** by an ethoxy moiety was unfavorable and compound **24** showed decreased potency (**24**, EC_{50} = 270 nM vs **23**, EC_{50} = 120 nM). Pleasingly, $mGlu_2$ PAM activity was significantly improved by the introduction of a trifluoromethyl group at the 5 position of the benzimidazolone scaffold (**25**) resulting in ~3.4-fold increase in potency compared to the unsubstituted analogue **24** (**25**, EC_{50} = 80 nM vs **24**, EC_{50} = 270 nM) and excellent metabolic stability in human and rat liver microsomes (HLM = 4% and RLM = 12%). Interestingly, the pyrimidine analogue **26** displayed comparable activity to **25** and no metabolites could be seen after incubation with HLM and RLM.

Table 2. Functional activity and metabolic stability data for representative 3-(azetidin-3-yl)-1*H*-benzimidazol-2-one $mGluR_2$ PAMs 21 -26[a].

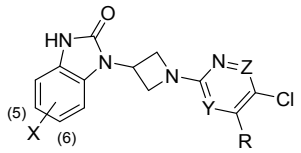

comp	X	R	Y	Z	$mGlu_2$ EC_{50}[a] (nM) (95% CI)	$mGlu_2$ E_{MAX} (%)[b] ± SD	HLM (%)[c]	RLM (%)[c]
21	6-Br	NHEt	CH	N	230 (200-262)	241 ± 71	9	26
22	H	NHEt	CH	N	280 (229-345)	291 ± 43	0	23
23	H	NHEt	CH	CH	120 (97-160)	381 ± 80	27	88
24	H	OEt	CH	CH	270 (202-368)	259 ± 38	15	46
25	5-CF_3	OEt	CH	CH	80 (57-113)	218 ± 32	4	12
26	5-CF_3	OEt	N	CH	150 (130-189)	220 ± 16	BQL[d]	BQL[d]

a Values are the mean of at least two experiments and within confidence interval of >95%. b Values are the median of at least two experiments with standard deviation. c HLM and RLM data refer to % of compound metabolized after incubation with microsomes for 15 min at a 5 uM concentration. d Below Quantification Limit.

Based upon their overall in vitro profile (e.g. good balance between potency and metabolism) and with the aim to maximize the potential to identify suitable in vivo probes, compounds **19**, **20**, **21**, **22**, **24** and **25** were evaluated after oral dose in a PK study in rat and for their ability to cross the blood−brain barrier (BBB). Thus, plasma and brain levels measured 2 and 4 h after dosing at 10 or 30 mg/kg are shown in Table 3. With the exception of **19**, compounds display relevant plasma exposures after 4 hours administration reflecting low to moderate clearance, in line with the in vitro rat metabolism previously shown. Moreover, the brain penetration was generally low for most of the compounds with K_p values below 0.4, with the exception of compound **20** (K_p = 1.4). To rule out potential interaction with the glycoprotein P (P-gp), the efflux ratio of compounds **24** and **25** was evaluated in LLC-PK1 cell lines transfected with MDR1 showing no indication for P-gp efflux with values of 1.18 and 1.24 x 10^{-6} cm/s for both **24** and **25** respectively. Likewise, both compounds possessed moderate permeability (13 and 9 x 10^{-6} cm s for **24** and **25** respectively). Interestingly, the K_p values followed a trend with log P, excluding **25**, in which its higher lipophilicity, may not account for its poor brain penetration. Thus, for example, increasing the lipophilicity by replacing the chlorine atom in the pyridazine ring (**19**) by a trifluoromethyl group (**20**) led to an increase in K_p that translated into higher brain exposures. Conversely, the reduction of lipophilicity in compound **21** by removing the bromine atom on the benzimidazolone ring led to compound **22** which displayed lower K_p value. In view of these data, compounds **20**, **24** and **25** displayed the best combination of low plasma clearance and relevant brain concentrations maintained at least for 4 h.

In addition, all compounds displayed a high level of selectivity toward all mGlu receptor subtypes: $mGlu_1$ and $mGlu_{3-8}$ (see compound **20** as example in supporting information). Likewise, potential off-target interactions were explored in a limited CEREP panel containing 18 different targets and also in the DiscoverX kinase panel (see supporting information) showing overall clean selective profiles with the exception of A2B (IC_{50} 0.79 uM) for compound **20**.

Collectively, our data show that compounds **20**, **24** and **25** are suitable tools derived from novel templates to further explore the therapeutic potential of $mGlu_2$ PAMs in biological models of CNS disorders. In vivo studies to confirm their in vitro activity are in progress and will be reported in due course.

Table 3. Brain and Plasma kinetics in rat after a single oral dose.a

compd	Plasma level (ng/mL)		Brain level (ng/g)		K_p[b]	ALogP
	2 h	4 h	2 h	4 h	2 h	
19[c]	49	17	18	BQL[d]	0.37	2.94

20[c]	260	220	310	290	1.4	3.43
21[c]	254	416	18	18	0.07	2.64
22	1,480	842	48	31	0.03	1.9
24	5,770	5,780	2,050	2,374	0.36	2.14
25	2,660	5,090	371	996	0.14	3.1

[a] Study in male Sprague Dawley rat (n= 1) dosed at 30 mg/kg p.o. in suspension (20% HP-β-CD at pH 7). [b]K_p is partition coefficient between brain and plasma after 2 hours. [c]10 mg/kg dose p.o. [d] Below Quantification Limits.

CHEMISTRY

The general synthetic schemes for the preparation of spiro-oxindole piperidines (**6-20**) and 3-(azetidin-3-yl)-1H-benzimidazol-2-ones (**21-26**) are outlined in Scheme 1 and Scheme 2 respectively. The precursor compounds **27a-e**, **28a-d**, **28f** and **31a-b** were commercially available. For the preparation of compounds **6-20** the general procedure involves a nucleophilic aromatic substitution on a 3,6-dichoropyridazine heterocycle (**28a-g**) with the corresponding spirocyclic piperidine derivative (**27a-g**) using DIPEA or K_2CO_3 (Scheme 1) as base. The benzimidazole azetidines **21-26** were prepared following a similar reaction procedure, starting in this case from the corresponding benzimidazole derivative **31a-c** and chloro-heterocycle **28e**, **32a-c** (Scheme 2).

Scheme1. General synthesis of spiro-oxindole piperidines 6-20[a]

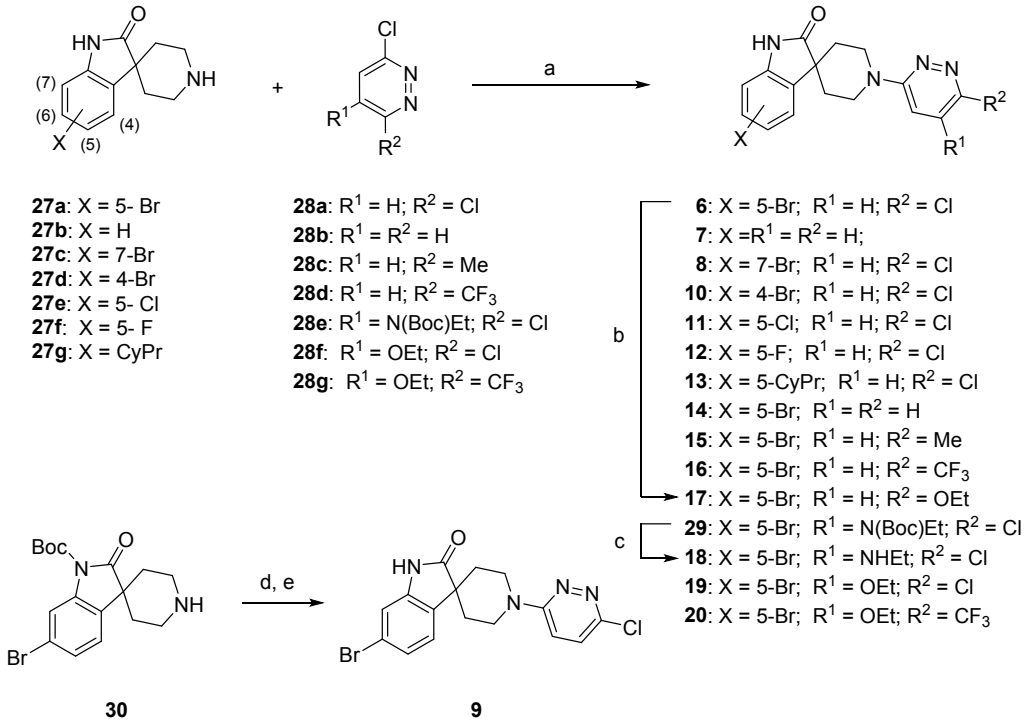

[a]Reagents and conditions: (a) DIPEA or K_2CO_3, solvent, 85 - 150 ºC. Y: 2 - 78%, see Supporting Information for detailed protocol; (b) NaOEt, EtOH, 0 to 100 ºC, 48h. Y: 40%; (c) TFA, DCM, rt, 1h. Y: 42%; (d) **28a**, CuI, DMEDA, K_2CO_3, DMF, 120 ºC, 12h; (e) HCl, MeOH, rt, 1h. Y: 5% (two steps)

Scheme2. General synthesis of 3-(azetidin-3-yl)-1*H*-benzimidazol-2-ones 21-26[a]

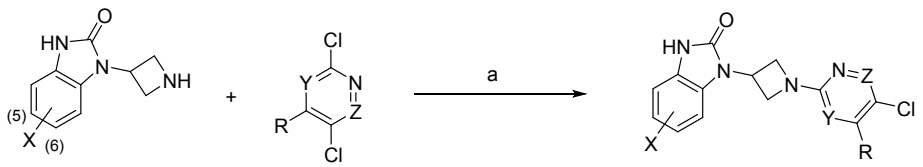

31a: X = 6-Br
31b: X = H
31c: X = 5-CF_3

28e: Y = CH; Z = N; R = N(Boc)Et
32a: Y = Z = CH, R = $CF_3C(O)NEt$
32b: Y = Z = CH, R = OEt
32c: Y = N; Z = CH, R = OEt

b → **33**: X = 6-Br; Y = CH; Z = N; R = N(Boc)Et
→ **21:** X = 6-Br; Y = CH; Z = N; R = NHEt
b → **34**: X = H; Y = CH; Z = N; R = N(Boc)Et
→ **22:** X = H; Y = CH; Z = N; R = NHEt
c → **35**: X = H; Y = Z = CH; R = $CF_3C(O)NEt$
→ **23:** X = H; Y = Z = CH; R = NHEt
24: X = H; Y = Z = CH, R = OEt
25: X = 5-CF_3; Y = Z = CH, R = OEt
26: X = 5-CF_3; Y = N; Z = CH, R = OEt

[a]Reagents and conditions: (a) DIPEA or K_2CO_3, solvent, 85 - 130 ºC. Y: 15 - 85%, see Supporting Information for detailed protocol; (b) TFA, DCM, rt, 1h. Y 32 - 39%; (c) K_2CO_3, MeOH, H_2O, 50 ºC, 4h. Y: 23%

CONCLUSIONS

In summary, we have outlined the medicinal chemistry strategies employed in the optimization of micromolar HTS hits to the identification of two novel $mGlu_2$ PAM series. A hybrid design approach that combined the two HTS hits gave quick access to a novel series that after systematic SAR studies including a scaffold hopping approach, delivered compounds with good in vitro potency, selectivity and appropriate pharmacokinetic attributes to progress to in vivo PD studies.

ASSOCIATED CONTENT

*Supporting Information

Assay protocols, experimental procedures, and analytical data for compounds **6-26**, **27f-g**, **28e**, **28g**, **29**, **30**, **31c**, **32a, 33, 34** and **35** (PDF)

AUTHOR INFORMATION

Corresponding Authors

*for A.I.L: phone, +34 925 245770; e-mail: adelucas@its.jnj.com
*for J.M.C: phone, +34 925 245767; e-mail: jcid@its.jnj.com.

Author Contributions

The manuscript was written through contributions of all authors. / All authors have given approval to the final version of the manuscript.

Notes

The authors declare no competing financial interest.

ACKNOWLEDGMENT

The authors thank Dr Manuela Ariza, Dr Miriam Ciordia and Dr María Morón for their synthetic contributions and members of the purification and analysis team from Toledo, the biology and ADMET team from Janssen R & D. The authors further thanks Ilse Biesmans for data management support.

ABBREVIATIONS

$mGlu_2$, metabotropic glutamate 2; PAM, positive allosteric modulator; GPCR, G protein-coupled receptor, CNS, central nervous system; HTS, high throughput screening; SAR, structure-activity relationship. RLM, rat liver microsomes; HLM, human liver microsomes.

REFERENCES

(1) Kew, J. N. C.; Kemp, J. A. Ionotropic and metabotropic glutamate receptor structure and pharmacology. *Psychopharmacology* **2005**, *179*, 4−29.

(2) Pin, J. P.; Galvez, T.; Prezeau, L. Evolution, structure, and activation mechanism of family 3/C G-protein-coupled receptors. *Pharmacol. Ther.* **2003**, *98*, 325−354.

(3) Braeuner-Osborne, H.; Wellendorph, P.; Jensen, A. A. Structure, pharmacology and therapeutic prospects of family C G-protein coupled receptors. *Curr. Drug Targets* **2007**, *8*, 169-184.

(4) Szabo, G.; Keseru, G. M.; Positive allosteric modulators for mGlu2 receptors: a medicinal chemistry perspective. *Curr. Top. Med. Chem.* **2014**, *14*, 1771-1788.

(5) Trabanco A. A.; Cid, J. mGluR2 positive allosteric modulators: a patent review (2009 - present). *Expert Opin: Ther. Pat.* **2013**, *23*, 629-647.

(6) Trabanco, A. A.; Cid, J. M.; Lavreysen, H.; Macdonald, G. J.; Tresadern, G. Progress in the development of positive allosteric modulators of the metabotropic glutamate receptor 2. *Curr. Med. Chem.* **2011**, *18*, 47-68.

(7) Metcalf, C. S.; Klein, B. D.; Smith, M. D.; Pruess, T.; Ceusters, M.; Lavreysen, H.; Pype, S.; Van Osselaer, N.; Twyman, R.; White, H. S. Efficacy of mGlu2-positive allosteric modulators alone and in combination with levetiracetam in the mouse 6 Hz model of psychomotor seizures *Epilepsia* **2017**, *58*, 484–493;

(8) Metcalf, C. S.; Klein, B. D.; Smith, M. D.; Pruess, T.; Ceusters, M.; Lavreysen, H.; Pype, S.; Van Osselaer, N.; Twyman, R.; White, H. S. Potent and selective pharmacodynamic synergy between the metabotropic glutamate receptor subtype 2–positive allosteric modulator JNJ-46356479 and levetiracetam in the mouse 6-Hz (44-mA) model. *Epilepsia* **2018**, *59*, 724–735.

(9) Lavreysen, H.; Langlois, X.; Ver Donck, L.; Cid Nuñez, J. M.; Pype, S.; Lütjens, R.; Megens, A. Preclinical evaluation of the antipsychotic potential of the mGlu2-positive allosteric modulator JNJ-40411813. *Pharmacol. Res. Perspect.* **2015**, *3*, e00097.

(10) Salih, H.; Anghelescu, I.; Kezic, I.; Sinha, V.; Hoeben, E.; Van Neuten, L.; De Smedt, H.; De Boer, P. Pharmacokinetic and pharmacodynamic characterization of JNJ-40411813, a positive allosteric modulator of $mGluR_2$, in two randomised, double-blind phase-I studies. *J. Psychopharmacol.* **2015**, *29*, 414-425.

(11) Cid, J. M.; Duvey, G.; Tresadern, G.; Nhem, V.; Funary, R.; Cluzeau, P.; Vega, J. A.; de Lucas, A. I.; Matesanz, E.; Alonso, J. M.; Linares, M. L.; Andres, J. I.; Poli, S.; Lutjens, R.; Imogai, H.; Rocher, J.- P.; MacDonald, G. J.; Oehlrich, D.; Lavreysen, H.; Ahnaou, A.; Drinkenburg, W.; Mackie, C.; Trabanco, A. A. Discovery of 1,4-disubstituted 3-cyano-2-pyridones: a new class of positive allosteric modulators of the metabotropic glutamate 2 receptor. *J. Med. Chem.* **2012**, *55*, 2388−2405.

(12) Cid, J. M.; Tresadern, G.; Duvey, G.; Lutjens, R.; Finn, T.; Rocher, J.-P.; Imogai, H.; Poli, S.; Vega, J.; de Lucas, A. I.; Matesanz, E.; Linares, M. L.; Andrés, J. I.; Alcazar, J.; Macdonald, G. J.; Oehlrich, D.; Lavreysen, H.; Ahnaou, A.; Drinkenburg, W.; Mackie, C.; Pype, S.; Gallacher, D.; Trabanco, A. A. Discovery of 1-butyl-3-chloro-4-(4-phenyl-1-piperidinyl)-(1H)-pyridone (JNJ-40411813): a novel positive allosteric modulator of the metabotropic glutamate 2 receptor *J. Med. Chem.* **2014**, *57*, 6495-6512.

(13) Tresadern, G.; Cid, J. M; Macdonald, G. J.; Vega, J. A.; de Lucas, A. I.; García, A.; Matesanz, E.; Linares, M. L.; Oehlrich, D.; Lavreysen, H.; Biesmans, I.; Trabanco, A. A. Scaffold hopping from pyridones to imidazo[1,2-a]pyridines. New positive allosteric modulators of metabotropic glutamate 2 receptor. *Bioorg. Med. Chem. Lett.* **2010**, *20*, 175−179.

(14) Trabanco, A. A.; Tresadern, G.; Macdonald, G. J.; Vega, J. A.; de Lucas, A. I.; Matesanz, E.; García, A.; Linares, M. L.; Alonso de Diego, S: A.; Alonso, J. M.; Oehlrich, D.; Ahnaou, A.; Drinkenburg, W.; Mackie, C.; Andrés, J. I.; Lavreysen, H.; Cid J. M. Imidazo[1,2-a]pyridines: orally active positive allosteric modulators of the metabotropic glutamate 2 receptor. *J. Med. Chem.* **2012**, *55*, 2688-2701.

(15) Cid, J. M.; Tresadern, G.; Vega, J. A.; De Lucas, A. I.; Matesanz, E.; Iturrino, L.; Linares, M. L.; García, A.; Andrés, J. I.; Macdonald, G. J.; Oehlrich, D.; Lavreysen, H.; Megens, A.; Ahnaou, A.; Drinkenburg, W.; Mackie, C.; Pype, S.; Gallacher, D.; Trabanco, A. A. Discovery of 3-cyclopropylmethyl-7-(4-phenyl-piperidin-1-yl)-8-trifluoromethyl-[1,2,4]triazolo[4,3-a] pyridine (JNJ-42153605): A positive allosteric modulator of the metabotropic glutamate 2 receptor. *J. Med. Chem*. **2012**, *55*, 8770−8789.

(16) Cid, J. M.; Tresadern, G.; Vega, J. A.; de Lucas, A. I.; del Cerro, A.; Matesanz, E.; Linares, M. L.; García, A.; Iturrino, L.; Pérez-Benito, L.; Macdonald, G. J.; Oehlrich, D.; Lavreysen, H.; Peeters, L.; Ceusters, M.; Ahnaou, A.; Drinkenburg, W.; Mackie, C.; Somers, M. and Trabanco, A. A. Discovery of 8-trifluoromethyl-3-cyclopropylmethyl-7-[(4-(2,4-difluorophenyl)-1-piperazinyl)methyl]-1,2,4-triazolo[4,3-a]pyridine (JNJ-46356479), a selective and orally bioavailable mGlu2 receptor positive allosteric modulator (PAM). *J. Med. Chem.* **2016**, *59*, 8495−8507.

(17) Farinha, A.; Lavreysen, H.; Peeters, L.; Russo, B.; Masure, S.; Trabanco, A. A.; Cid, J.; Tresadern, G. Molecular determinants of positive allosteric modulation of the human metabotropic glutamate receptor 2 Br. J. Pharmacol. 2015, 172, 2383– 2396.

(18) Doornbos, M. L.; Wang, X.; Vermond, S. C.; Peeters, L.; Pérez-Benito, L.; Trabanco, A. A.; Lavreysen, H.; Cid, J. M.; Heitman, L. H.; Tresadern, G.; IJzerman, A. P. Covalent allosteric probe for the metabotropic glutamate receptor 2: design, synthesis, and pharmacological characterization. *J. Med. Chem.* **2019**, *62*, 223– 233.

(19) Pérez-Benito, L.; Doornbos, M. L. J.; Cordomí, A.; Peeters, L.; Lavreysen, H.; Pardo, L.; Tresadern, G. Molecular switches of allosteric modulation of the metabotropic glutamate 2 receptor. *Structure* **2017**, *25*, 1153– 1162.

(20) Tresadern, G.; Bemporad, D.; Howe, T. A comparison of ligand based virtual screening methods and application to fcorticotropin releasing actor 1 receptor *J. Mol. Graphics Modell.* **2009**, *27*, 860– 870.

(21) Hawkins, P.C.D.; Skillman, A.G. and Nicholls, A., Comparison of Shape-Matching and Docking as Virtual Screening Tools, Journal of Medicinal Chemistry, Vol. 50, pp. 74-82, 2007.

(22) ROCS version 3.2.0.4, EON version 2.2.0.5: OpenEye Scientific Software. Santa Fe, NM, 2013.